

SONY

Want to see all
the colors?

*The choice is black
and silver.*



FP7000 Spectral Cell Sorter



ID7000™ Spectral Cell Analyzer

The Journal of Immunology

RESEARCH ARTICLE | AUGUST 15 2005

CC Chemokine Ligand 19 Secreted by Mature Dendritic Cells Increases Naive T Cell Scanning Behavior and Their Response to Rare Cognate Antigen **FREE**

Andrew Kaiser; ... et. al

J Immunol (2005) 175 (4): 2349–2356.

<https://doi.org/10.4049/jimmunol.175.4.2349>

Related Content

Cutting Edge: Atypical PKCs Regulate T Lymphocyte Polarity and Scanning Behavior

J Immunol (November,2007)

Mapping Interaction Sites on Human Chemokine Receptors by Deep Mutational Scanning

J Immunol (June,2018)

Antigen Availability and DOCK2-Driven Motility Govern CD4⁺ T Cell Interactions with Dendritic Cells In Vivo

J Immunol (July,2017)

CC Chemokine Ligand 19 Secreted by Mature Dendritic Cells Increases Naive T Cell Scanning Behavior and Their Response to Rare Cognate Antigen

Andrew Kaiser,* Emmanuel Donnadieu,[†] Jean-Pierre Abastado,* Alain Trautmann,[†] and Alessandra Nardin^{1*}

For immune responses to take place, naive T cells have to encounter, adhere to, and be stimulated by dendritic cells (DCs). In murine lymph nodes, T cells move randomly and scan the surface of multiple DCs. The factors controlling this motility as well as its consequences remain unclear. We have monitored by video-imaging the earliest steps of the interaction between human DCs and autologous naive CD4⁺ T cells in the absence of exogenous Ags. Mature, but not immature, DCs were able to elicit small calcium responses in naive T cells along with cell polarization and random motility, resulting in an efficient scanning of DC surfaces by T cells. We identified CCL19 as a key factor enabling all these early T cell responses, including the occurrence of calcium transients. Because this chemokine did not influence the strength of naive T cell adhesion to DCs, enhanced LFA-1 affinity for ICAM-1 was not the main mechanism by which CCL19 increased Ag-independent calcium transients. However, concomitantly to T cell motility, CCL19 augmented the frequency of T cell responses to rare anti-CD3/CD28-coated beads, used as surrogate APCs. We thus propose a new role for CCL19 in humans: by conditioning T cells into a motile DC-scanning state, this chemokine promotes Ag-independent responses and increases the probability of cognate MHC-peptide encounter. *The Journal of Immunology*, 2005, 175: 2349–2356.

Dendritic cells (DCs)² are the most potent APCs and can be found in most tissues. Upon maturation, they migrate to draining lymph nodes where they prime naive T cells because of their ability to express, in a combined and regulated manner, high levels of Ag-presenting molecules, costimulatory and adhesion molecules, cytokines, and chemokines (1). To enter the lymph nodes, naive T cells are guided by integrins and chemokines, in particular the CCR7 ligands: CCL19 (also known as EBV-induced gene 1 ligand chemokine or MIP-3 β) and CCL21 (also known as secondary lymphoid tissue chemokine, exodus 2, or 6CKine). The latter is expressed on the luminal surface of high endothelial venules (HEVs), whereas both chemokines are secreted by stromal cells in the T cell areas of lymph nodes (2, 3). Experiments in *plt/plt* mice (paucity of lymph node T cells), deficient in CCL19 and CCL21, demonstrated their essential role in the entry of naive T cells into the lymph nodes (3, 4). In the T cell areas, few specific naive T cells must interact with important numbers of DCs to be able to respond to the low levels of presentation of their cognate antigenic peptide. Once activated, T cells are redirected to the peripheral tissues to exert their function.

The dynamics of interaction between mature DCs (mDCs) and T cells have been analyzed both *in vitro* and *in vivo*. Recently, *in vivo* two-photon microscopy in intact murine lymph nodes has

shown naive T cells to be very motile ($\sim 8 \mu\text{m}/\text{min}$) with a median T/DC interaction time of 3.8 min in the absence of Ag (5–7). It was calculated that DCs can be scanned by 500–5000 T cells/h (6, 8). However, it is not clear which factors are responsible for these very dynamic interactions between naive T cells and DCs. In addition, it is not known how this motility influences T cell responses.

To give some elements of response to these questions, we used an *in vitro* video-imaging system and studied the early responses induced by human monocyte-derived DCs on autologous naive CD4⁺ T cells in the absence of exogenous Ag. We have previously shown that immature DCs (iDCs) induce rapid polarization and random motility of memory T cells together with Ag-independent intracellular calcium (Ca²⁺) transients (9). Ag-independent Ca²⁺ responses have been correlated with prolonged T cell survival (10, 11). The current study shows that only mDCs are able to induce such a polarized and motile state in naive T cells, essentially due to an important secretion of CCL19. As a consequence of the crawling/scanning behavior of naive T cells triggered by this chemokine, interactions with APCs are optimized, leading to a higher frequency of Ag-independent Ca²⁺ responses, and favoring T cell encounters with rare cognate Ag.

Materials and Methods

Purification of T lymphocytes and generation of DCs

Human naive CD4⁺ T cells were purified from PBMCs of healthy volunteers by negative selection using CD4⁺ T cell isolation kit (Miltenyi Biotec) according to the manufacturer's instructions. CD45RO Microbeads were added during isolation. The purity of viable CD4⁺ CD45RO⁺ T cells obtained was >93%. DC differentiation was performed with VACCELL processor (IDM) as previously described (12, 13). Briefly, PBMCs were cultured for 7 days in serum-free VACCELL medium (Invitrogen Life Technologies) supplemented with 500 U/ml GM-CSF (Novartis Pharma) and 50 ng/ml IL-13 (Sanofi-Synthelabo). DCs were then isolated by elutriation. Purity ranged from 80 to 99%; viability was >95%. In some instances, DCs were frozen in a solution of 4% human albumin containing

*Immuno-Designed Molecules (IDM), Paris, France; and [†]Institut Cochin Centre National de la Recherche Scientifique-Institut National de la Santé et de la Recherche Médicale, Paris, France

Received for publication February 25, 2005. Accepted for publication May 30, 2005.

The costs of publication of this article were defrayed in part by the payment of page charges. This article must therefore be hereby marked *advertisement* in accordance with 18 U.S.C. Section 1734 solely to indicate this fact.

¹ Address correspondence and reprint requests to Dr. Alessandra Nardin, IDM, Institut Biomédical des Cordeliers, 15 rue de l'École de Médecine, 75006 Paris, France. E-mail address: anardin@idm-biotech.com

² Abbreviations used in this paper: DC, dendritic cell; HEV, high endothelial venule; iDC, immature DC; mDC, mature DC; PTX, pertussis toxin.

10% DMSO, then matured after thawing and overnight recovery. For maturation, 2×10^6 DCs/ml were cultured in 24-well plates for 20 h in the presence of $1 \mu\text{g/ml}$ bacterial extract (FMKp; Pierre Fabre Medicament) and 500 U/ml IFN- γ (Imukin; Roche). For experiments using supernatants, the culture medium of DCs matured for 20 h was used. The DCs used in this work have been previously thoroughly described (12, 13). They present a classical phenotype of monocyte-derived DCs and up-regulate CD83, B7 molecules, CD40, CD25, and MHC molecules after maturation.

Single-cell video imaging

Measurement of the intracellular Ca^{2+} concentration was performed as previously described (14). Briefly, DCs were washed with mammalian saline buffer, and 1.5×10^5 cells were left to adhere to glass coverslips for 15 min at 37°C . Nonadherent cells were removed by two gentle washes with the buffer supplemented with 2% autologous human serum. In parallel, 4×10^5 T cells were incubated for 20 min at 37°C with $1 \mu\text{M}$ fura 2-AM (Molecular Probes), washed, and added to the DC layer. When indicated, T cells were pretreated overnight with 50 ng/ml pertussis toxin (PTX; Calbiochem). Image acquisitions were performed in a final volume of $100 \mu\text{l}$. DC culture supernatant was added at a final dilution of 1/2. In some experiments, monolayers of DCs or mDC culture supernatant were incubated with $10 \mu\text{g/ml}$ of the following Abs for 20 min at 37°C before T cell addition: neutralizing anti-CCL19 or anti-CCL18 Abs, total goat IgG as control (R&D Systems), or blocking anti-ICAM-1 mAb (clone HA58; BD Biosciences). In some cases, after staining with fura 2-AM, T cells were incubated for 20 min at 37°C with $10 \mu\text{g/ml}$ blocking anti-CCR7 or anti-CXCR4 mAbs (clones 150503 and 44716, respectively; R&D Systems). In some experiments on T/DC contact, 2×10^4 anti-CD3/anti-CD28-coated beads ($5\text{-}\mu\text{m}$ diameter; Dynal Biotech) were used as surrogate APCs. Beads were washed and added in $10 \mu\text{l}$ of buffer to the monolayer of DCs before naive T cells addition. Imaging was performed with an Eclipse TE300 (Nikon) inverted microscope, equipped with a $\times 60$ UV-permissive objective, in a 37°C regulated chamber. Images were obtained with a cooled charge-coupled device camera (CoolSNAPfx; Roper Scientific) and the Metafluor acquisition imaging software (Universal Imaging). Fura 2-AM-loaded cells were excited at 350 and 380 nm. Emission at 510 nm and transmitted light were used for analysis of Ca^{2+} responses. Intracellular Ca^{2+} concentrations were calculated with the equation reported by Gryniewicz et al. (15). The values of the fluorescence ratios, R_{min} and R_{max} , were 0.8 and 15, respectively. All experimental conditions were tested in duplicate.

Quantification of T cell polarization, motility, and Ca^{2+} responses

T cell polarization was quantified by visual inspection of cell morphology after exposure to 200 ng/ml rCCL19 (R&D Systems), DC culture supernatant, or DCs. T cells were considered polarized upon acquisition of an elongated shape with active membrane processes sustained over 1 min. T cells movements were tracked, and the maximum distance traveled in 10 min from the origin was determined using Metamorph software (Universal Imaging). The frequency of motile T cells was calculated as the fraction of T cells moving of at least $10 \mu\text{m}$ from their origin within the 20 min of recording. Ca^{2+} responses were assessed with Metafluor software (Universal Imaging). The responses with amplitudes at least twice that of the background (T cells in the absence of DCs) were considered positive.

Adhesion assay

Ag-independent adhesion between DCs and autologous naive CD4^+ T cells was quantified as follows. DCs (4×10^5) were plated for 15 min on glass slides in the presence or the absence of $10 \mu\text{g/ml}$ anti-CCL19 or anti-ICAM-1 blocking Abs. Cells were then washed, and the glass slide was assembled in a parallel-plate laminar flow chamber (Immunetics). The flow chamber was mounted on the microscope equipped with a $\times 20$ objective. T cells (5×10^5) were loaded for 5 min with $2.5 \mu\text{M}$ CFSE (Molecular Probes), washed, incubated, or not, for 20 min at 37°C with anti-CCR7 and anti-CCL19 blocking Abs, and infused in the chamber. To measure the percentage of cells adhering to the DC monolayer, images were acquired every 5 s. First, a constant flow of 1 ml/h (0.05 dyn/cm^2) of mammalian saline buffer plus 2% autologous serum was applied for 8 min. Then, after 7 min of T-DC adhesion under static conditions at 37°C , increasing flow rates (from 0.05 to 4 dyn/cm^2) were applied. The percentage of T cells remaining adherent to DCs was scored from processed fluorescent images acquired during the experiment.

ELISA

CCL19 in supernatants of 20-h DC culture was quantified by ELISA using Ab pairs from R&D Systems according to the manufacturer's instructions.

Semiquantitative RT-PCR

The protocol was reported previously (9). Briefly, total RNA from 10^6 iDC and 20-h mDCs (purity $>95\%$) was extracted using TRIzol reagent (Invitrogen Life Technologies). cDNA was prepared using Moloney murine leukemia virus reverse transcriptase and oligo(dT) primers from the Advantage RT-for-PCR kit (BD Biosciences). PCR cycling conditions were as follows: denaturation at 94°C for 45 s, annealing at 60°C for 45 s, and extension at 72°C for 60 s (25 and 30 cycles). PCR products were resolved on a 1% agarose gel containing ethidium bromide.

Statistical analysis

A one-tailed Mann-Whitney nonparametric test was used for all statistical analysis. A value of $p \leq 0.05$ was considered significant.

Results

mDCs induce strong polarization, motility, and Ag-independent Ca^{2+} responses in naive T cells

We used a video-microscopy system to define some of the early responses of naive T cells to immature or mature DCs. Human naive $\text{CD4}^+ \text{CD45RO}^-$ T cells were cocultured on glass coverslips with autologous monocyte-derived DCs. The culture of DCs in serum-free medium without addition of exogenous Ag allowed us to study Ag-independent interactions.

In the presence of iDCs, naive T cells displayed a passive behavior; they stayed round, not motile, and had very few interactions with iDCs (Fig. 1a and supplemental material, video 1).³ We observed only minor displacements of the T cells, mostly due to Brownian motion. In contrast, naive T cells in the presence of mDCs underwent rapid and important changes in their morphology, acquiring a torpedo shape with a leading edge and a trailing uropod. This polarization, generally sustained during the 20 min of imaging, was also observed when using the culture supernatant of mDCs (Fig. 1b and supplemental material, video 2), indicating that the polarizing factor was secreted. An average of 60% naive T cells became polarized in the presence of mDCs or mDC supernatant vs 10% with iDCs or their culture supernatant.

The tracking of naive T cells on a monolayer of mDCs also revealed a higher motility compared with that observed on a monolayer of iDCs (Fig. 1c). The average frequency of motile T cells in the presence of mDCs was 42.1 ± 14.8 vs $10.7 \pm 9.3\%$ in the presence of iDCs ($n = 5$). T cell motility appeared random, similar to what was previously reported *in vivo* in lymph nodes (6). Mean T cell velocity on mDCs was $7.7 \pm 0.1 \mu\text{m/min}$ (average of 20 cells from three independent experiments), with peaks at $57 \mu\text{m/min}$.

Measuring the maximum distance of migration from the origin, we observed that naive T cells in the presence of mDCs travel at least four times further than in the presence of iDCs (Fig. 1d). Thus, by increasing the frequency of motile T cells as well as their traveling distances, mDCs enable naive T cells to scan a large number of APCs.

It was previously described that DCs can induce weak transient Ca^{2+} responses in T cells even in the absence of exogenous Ag (9, 11, 16). Therefore, we measured the frequency of Ag-independent Ca^{2+} responses obtained in human naive T cells upon contact with autologous DCs. During the 12 min of image acquisition, mDCs were able to induce small Ca^{2+} transients in 15–30% of T cells, three to five times more than with iDCs. These Ag-independent Ca^{2+} responses were characterized by repetitive small increases

³ The online version of this article contains supplemental material.

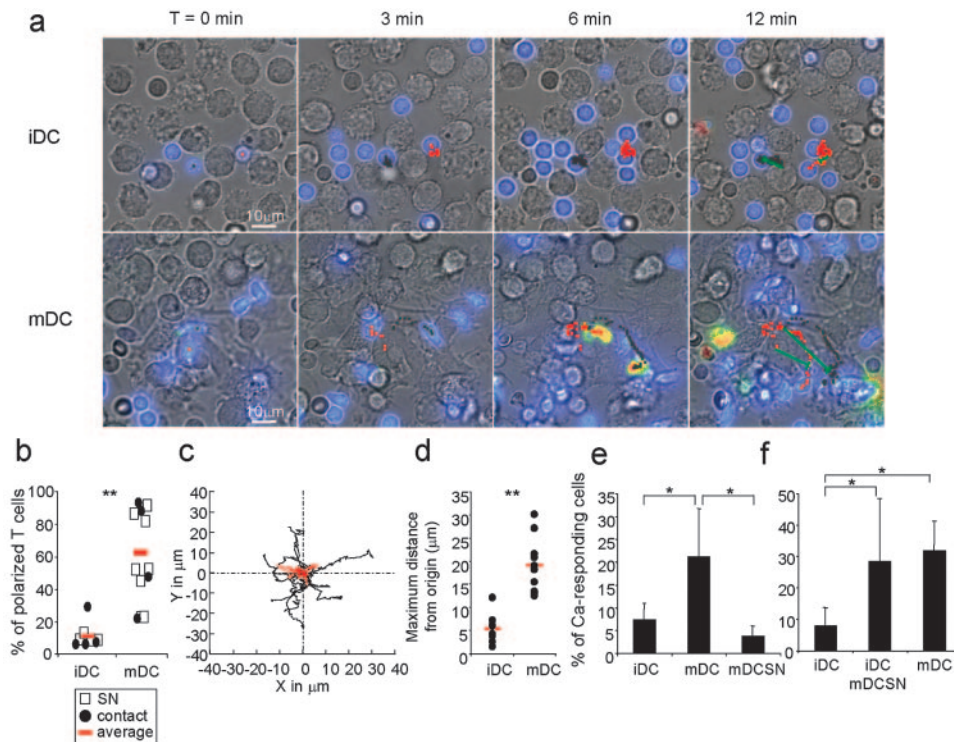


FIGURE 1. Mature DCs induce polarization, motility, and Ag-independent Ca^{2+} responses in naive T cells. Immature or mature DCs (10^5) were placed on glass coverslips to adhere for 15 min at 37°C and then washed. Naive T cells (5×10^5) loaded with fura 2-AM were added before image recording. Images were recorded every 10 s for 12 to 20 min. *a*, Behavior of T cells in contact with either iDCs or mDCs. The T cell Ca^{2+} level is coded in color, ranging from blue to red. Black and red dots represent the tracking of T cell movements, and green bars represent the maximum distance traveled from the origin in 12 min. See also supplemental material, videos 1 and 2. *b*, Percentage of polarized T cells defined visually within 15 min of recording. Squares correspond to incubation of naive T cells with 20-h culture supernatant (SN) of DCs, and dots correspond to contact experiments in which T cells were coincubated with iDCs or mDCs. Averages of both conditions are shown as red bars. *c*, Motility tracks of 10 individual T cells coincubated with either iDCs (red lines) or mDCs (dark lines) for 15 min. Origins are merged. *d*, Distance from origin traveled by the cells shown in *c* (corresponding to the green bars shown in *a*). Red bars indicate average distance. *a*, *c*, and *d* are representative of six experiments. *e* and *f*, Average percentage of Ca^{2+} -responding T cells from four independent experiments \pm SD. Naive T cells coincubated with iDCs, mDCs, mDC 20-h culture supernatant (mDCSN), or iDCs plus mDCSN were monitored for 20 min. *, $p \leq 0.05$; **, $p < 0.0005$.

that usually did not exceed 400 nM (data not shown). The frequency of Ca^{2+} -responding cells depended on the time of acquisition. Indeed, we observed up to 74% of Ca^{2+} -responding cells when acquisition lasted 1 h (data not shown). Supernatant from mDC culture was unable to induce Ca^{2+} transients above the background ($\sim 5\%$, due to T cell adhesion to the glass; Fig. 1*e*), thus showing the contact dependence of such responses. Interestingly, however, the presence of mDC culture supernatant allowed for increased T cell responsiveness during contact with iDCs (Fig. 1*f*). Therefore, the ability of naive T cells to undergo Ca^{2+} transients relies on a soluble signal secreted by mDCs and does not appear to be influenced by the levels of costimulatory and adhesion molecules displayed by the DCs with which they interact.

CCL19 secretion by mDC induces early responses in naive T cells

We then evaluated which factor secreted by mDCs may account for the early responses observed. Chemokines are soluble factors able to trigger polarization and motility in a wide variety of cells. PTX ADP-ribosylates and inactivates the α subunit of the heterotrimeric G proteins used by most chemokine receptors to transmit their intracellular signals. We used PTX to study the role of chemokines in the T cell responses induced by mDCs.

PTX significantly inhibited mDC-induced T cell polarization and motility, resulting in diminished T cell traveling distances (Fig. 2, *a–c*). More surprisingly, blockage of the chemokine sig-

naling pathway also reduced to the level of iDCs the frequency of T cell Ca^{2+} responses induced by mDCs.

CCL18, CCL19, CCL21, and CXCL12 have all been reported to bind to chemokine receptors expressed on naive T cells (17, 18). To define the chemokines that may play a role in our system, we measured by RT-PCR their gene expression in DCs before and after maturation. CCL18 was detected in both the immature and the mature state, whereas CCL19 appeared exclusively after maturation (Fig. 3*a*). No mRNAs for CCL21 or CXCL12 were observed in DCs before and after maturation even after 30 cycles of PCR amplification, in agreement with previous findings (19–21). ELISA measurements confirmed the presence of CCL19 in the 20-h culture supernatant of mDCs (average, 11.3 ± 8.2 ng/ml; $n = 7$).

Neutralizing Abs were next used to define the mDC-derived chemokines inducing early T cell responses. T cell polarization initiated by mDC supernatant was reduced by $>92\%$ in the presence of anti-CCR7 or anti-CCL19 Abs, whereas anti-CCL18 Abs had no effect (Fig. 3*b*). In contact experiments, the reduction of T cell polarization by anti-CCR7 or anti-CCL19 Abs amounted to 70 and 55%, respectively. The local secretion of CCL19 within the synaptic apposition of T cell and DC membranes may explain this partial inhibition. Moreover, in contact, some costimulatory and/or adhesion molecules could synergize with the chemokines, thus decreasing the blocking effect of the Abs.

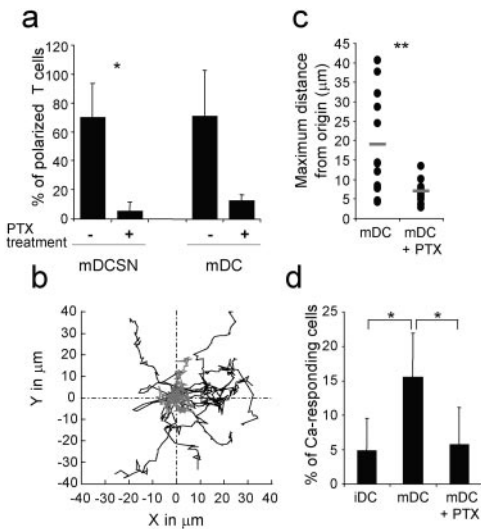


FIGURE 2. Early naive T cell responses are driven by mDC-secreted chemokines. Naive T cells were incubated, or not, with 50 ng/ml PTX overnight before 20-min video acquisition in the presence of DCs or mDC culture supernatant (mDCSN). *a*, Blocking effect of PTX on the percentage of polarized T cells incubated with mDCs or mDCSN (average of three experiments \pm SD). *b*, Motility tracks of 10 T cells on a monolayer of mDCs (15-min measurement) with (gray lines) or without (dark lines) PTX treatment. *c*, Quantification of the maximum distance traveled from the origin by the cells shown in *b*. Gray bars indicate the average distance. *d*, Effect of PTX on the percentage of Ca^{2+} -responding T cells incubated with mDC (average of three experiments \pm SD). *, $p \leq 0.05$; **, $p < 0.005$.

Blocking experiments indicated that the random T cell motility induced by mDCs was also essentially dependent on CCL19 (Fig. 3c). The mean maximal distance covered by naive T cells on a layer of mDCs was reduced 67% by Abs against CCR7 and CCL19 (Fig. 3d). In these experimental conditions, T cells traveled $>7.9 \pm 2.6 \mu\text{m}$ from their origin within 20 min, a distance similar to that observed on a monolayer of iDCs ($5.4 \pm 3 \mu\text{m}$; Fig. 1d).

Importantly, the anti-CCL19 Ab decreased the frequency of Ca^{2+} responses induced in T cells by mDCs as efficiently as PTX (Fig. 2d). In our system, therefore, CCL19 is the only chemokine responsible for the difference in frequency of Ca^{2+} responses induced in naive T cells by mDCs and iDCs (Fig. 3e).

Thus, these results suggest that CCL19 is relevant for the induction of a motile behavior facilitating the interaction between naive T cells and APCs and for the occurrence of Ca^{2+} responses upon such interaction.

CCL19 does not significantly affect adhesion of naive T cells to DCs under flow

The fact that the frequency of Ag-independent Ca^{2+} responses induced by mDCs is reduced upon abrogation of CCL19 signaling could be due to the decreased T cell motility and subsequently fewer interactions with APCs. Alternatively, it may be a consequence of suboptimal T cell adhesion to APCs. Indeed, chemokines can activate integrins such as LFA-1 (2) and therefore increase the strength of T cell interaction with cells expressing the ligands ICAM-1 (e.g., DCs) (9), ICAM-2, and ICAM-3.

Using a laminar flow chamber with the protocol summarized in Fig. 4, we assessed the role of mDC-secreted CCL19 on the ability of naive T cells to adhere to a layer of immature or mature DCs under a low constant flow of 0.05 dyn/cm^2 . After waiting 7 min in the absence of flow for the contacts to stabilize, the strength of the established interactions was studied by progressively increasing the shear forces to a flow of 4 dyn/cm^2 .

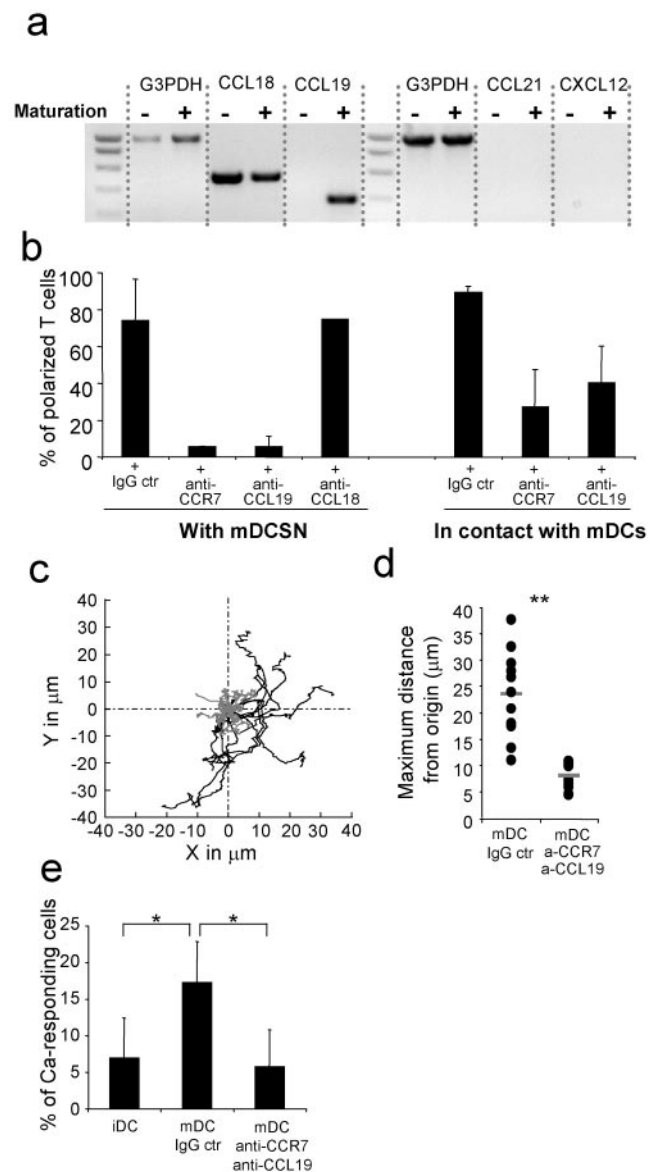


FIGURE 3. Mature DC-secreted CCL19 is the main chemokine inducing naive T cell polarization, motility, and Ca^{2+} responses. *a*, mRNAs of CCL18, CCL19, CCL21, CXCL12, and the housekeeping gene (G3PDH) in immature or 20-h matured DCs after 30 cycles of PCR (representative of two experiments). *b*, Abs against CCR7 and CCL19, but not anti-CCL18, decrease the percentage of T cells that become polarized after incubation with mDCs or mDCSN (from five independent experiments). *c*, Motility tracks of 10 T cells on a monolayer of mDCs (15-min measurement) in the presence of anti-CCR7 and anti-CCL19 blocking Abs (gray lines) or in the presence of IgG control Abs (dark lines; representative of four experiments). *d*, Maximum distance from the origin traveled by the cells shown in *c*. Gray bars indicate the average distance. *e*, Percentage of Ca^{2+} -responding T cells in contact with DCs with IgG control or anti-CCR7 and anti-CCL19 Abs (average of three experiments \pm SD). *, $p \leq 0.05$; **, $p < 0.0005$.

Under the initial weak constant flow, naive T cells adhered, on the average, two times more efficiently to mDCs than to iDCs (Fig. 4a). T cell adherence to mDCs was greatly reduced by anti-ICAM-1 blocking mAb, showing the importance of LFA-1/ICAM-1 interaction in the initial T/mDC adhesion step. Blocking CXCR4 had no effect on T cell adhesion to mDC, ruling out non-specific interference by steric hindrance of Abs bound to T cells. Blocking CCR7 signaling slightly inhibited these interactions in

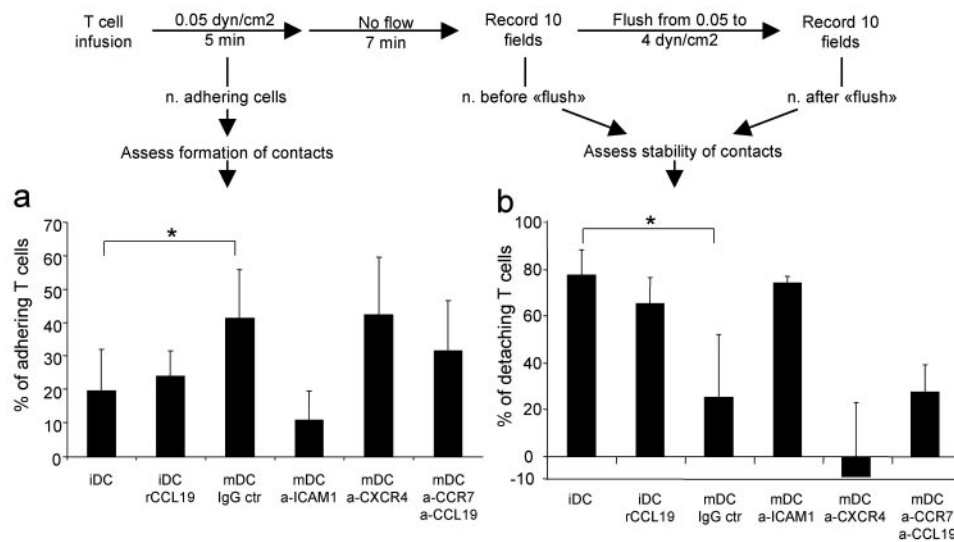


FIGURE 4. Under flow, CCL19 does not play a critical role in the adhesion of naive T cells to DCs. We used a laminar flow chamber to study the role of CCR7 signaling and ICAM-1 on the formation of naive T cell/DC contact and the stability of these interactions. The protocol used is represented above the histograms. *a*, Percentage of naive T cells adhering to DC, measured during infusion under weak constant flow on a monolayer of iDCs with or without rCCL19 or of mDCs with IgG control Abs or ICAM-1, CCR7, or CXCR4 blockage. *b*, Percentage of naive T cells detaching from DCs. T cells were left to adhere to the monolayer of DCs for 7 min, then a gradually increasing flow was applied to measure the percentage of detaching T cells. Data are the average \pm SD of three independent experiments. *, $p \leq 0.05$

some, but not all, experiments. This partial decrease was not statistically significant ($p = 0.183$). In addition, when incubating naive T cells with rCCL19, no significant increase in adhesion to iDCs could be observed (Fig. 4*a*).

By gradually increasing the flow after the T/DC contact had occurred, $77.3 \pm 11\%$ of the naive T cells were washed away from a monolayer of iDCs, whereas only $25.3 \pm 27\%$ detached from mDCs (Fig. 4*b*). This strong adhesion to mDC could be abrogated with anti-ICAM-1 Abs, but was not reduced by the control Ab to CXCR4. In this context, neither Abs blocking CCL19 signaling nor addition of rCCL19 showed an effect on the strength of T cell adhesion to, respectively, mDC or iDC (Fig. 4*b*).

Hence, in our experimental conditions, the adhesion molecule ICAM-1 is essential for stable interactions to take place between naive T cells and mDCs, but CCL19 does not appear to influence the initial adhesion or to affect the stability of the T/DC contact.

CCL19 increases the encounter of naive T cells with rare Ag-bearing APCs

Finally, we assessed whether the chemokinesis, crawling, and DC scanning behavior of naive T cells mediated by CCL19 increase the probability of encountering rare cognate Ags. We used 5- μ m diameter beads coated with anti-CD3 and anti-CD28 Abs as surrogate Ag-bearing APCs. The beads were added to a DC monolayer at a ratio of one bead per 7.5 DCs. This relatively high number of beads was necessary to reliably quantify T cell interactions with beads. The T cells encountering beads presented intense and long-lasting Ca^{2+} responses, similar to those observed after interacting with DCs loaded with Ag (22) (data not shown). However, compared with real APCs, the beads had the advantage of a minimum risk of Ag leakage, in addition to being homogenous and easy to follow in our experimental model.

In the presence of iDCs, $11.9 \pm 9.9\%$ of naive T cells were motile. The addition of mDC supernatant or rCCL19 increased the frequency of motile T cells up to, respectively, 39.8 ± 14 and $41.7 \pm 26.3\%$, the same level as in the presence of mDCs ($41.3 \pm 13.4\%$; Fig. 5*a*). As shown above, such increased T cell motility

was reduced by 50–75% by a combination of anti-CCR7 and anti-CCL19 Abs. The presence of beads did not impair the motility of the T cells, because the frequency of motile T cells with mDCs was comparable to that observed in previous experiments without beads ($42.8 \pm 17.8\%$ for mDCs vs $7.8 \pm 6.6\%$ for mDCs with blocking Abs).

In conditions where the signaling of CCL19/CCR7 was possible, the frequency of a productive encounter between naive T cells and the anti-CD3/anti-CD28 beads was three to four times higher than in the absence of CCL19/CCR7 signaling (Fig. 5*b* and supplemental material, videos 3 and 4). The frequency of Ca^{2+} responses on beads was generally higher on a monolayer of mDCs compared with iDCs plus mDC supernatant or plus rCCL19. A higher chemokine concentration or higher levels of costimulation and adhesion molecules on mDCs could explain this result. In the different experimental conditions, the frequency of motile T cells was directly correlated with the frequency of naive T cells responding to the beads after migration (Fig. 5*c*; $n = 3$ independent experiments).

Thus, this experimental model indicates that the acquisition of a motile crawling/scanning state induced by CCL19 increases the chances for naive T cells to encounter and interact with rare APCs bearing cognate Ag.

Discussion

The importance of CCR7 and its ligands CCL19 and CCL21 for the migration of naive T cells to lymphoid organs has been demonstrated in several *in vitro* and *in vivo* studies, mostly in mice. Lymph nodes of *plt/plt* mice and CCR7-deficient mice contain few naive T cells, but significant numbers of memory T cells. In addition, CCR7-deficient DCs fail to migrate from the skin into the lymphatic vessels (23, 24). Ngo et al. (25) demonstrated that CCL19 is expressed by DCs in the T cell zone and is a potent attractor of murine naive T cells. In the human system, we also observed CCL19-dependent, gradient-driven migration of T cells

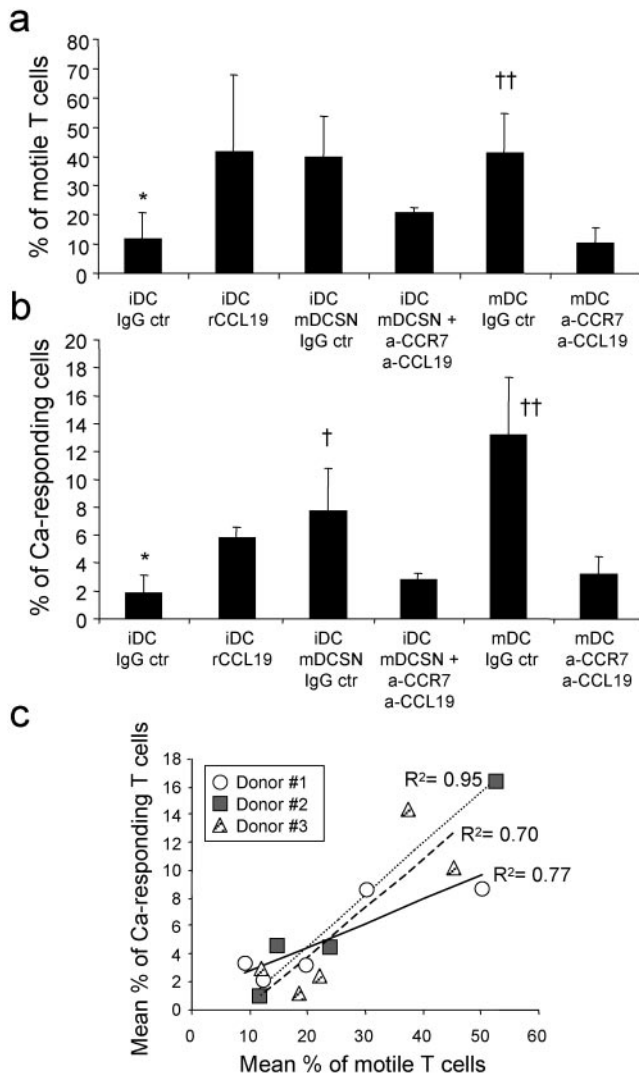


FIGURE 5. CCL19 increases the ability of naive T cells to encounter and interact with rare Ag-bearing APCs. Anti-CD3/anti-CD28-coated beads were added under the microscope to a monolayer of DCs (to a ratio of one bead per 7.5 DCs). After addition of naive T cells in the presence of IgG control or anti-CCR7 and anti-CCL19 Abs or rCCL19, we measured the percentage of T cells presenting a motile behavior (a) and the percentage of T cells showing Ca²⁺ responses to the beads after moving at least 10 μm (b). Data are the average ± SD of three experiments. See also supplemental material, videos 3 and 4. c, Correlation between the frequency of motile T cells and the frequency of naive T cells presenting Ca²⁺ responses to the beads, shown for each of the three independent experiments (all experimental conditions). *, $p \leq 0.05$ between iDC and iDC plus mDSCN or mDC; †, $p \leq 0.05$ between iDC plus mDSCN and iDC, mDSCN, anti-CCR7, plus anti-CCL19; ††, $p \leq 0.05$ between mDC and mDC, anti-CCR7, plus anti-CCL19.

to mature DC supernatant (not shown). Most importantly, however, we demonstrated that CCR7 signaling induces rapid and random T cell motility over a monolayer of DCs. This gradient-independent chemokinesis matched that observed in collagen gels (26) or in vivo in mice (5). Mean T cell velocities were similar (~8 μm/min). In the absence of cognate Ag, T/APC contacts were multiple and transient (5, 6). On the average, motile T cells interacted with up to 8 ± 3 DCs during the 20 min of image acquisition, and contacts as short as 30 s could lead to Ca²⁺ transients. This work extends previous observations on T cell/DC interactions to human cells and, in addition, identifies CCL19 as the sole factor

responsible for conditioning T cells into a motile DC-scanning state. More surprisingly, the small and transient Ca²⁺ increases induced in naive T cells by mDC in the absence of Ag were also dependent on CCL19. We thus propose that T cell polarization and motility promote Ag-independent Ca²⁺ responses while also increasing the probability of cognate MHC-peptide encounter. This hypothesis provides a mechanistic explanation for the results of a recent murine study in which CTL induction was abrogated by the injection of a CCL19 antagonist (27).

How does CCL19 affect T cell activation?

CCR7 signaling has been shown to increase the avidity of integrins such as LFA-1 for their ligands (2). CCL19 could therefore allow the formation of more stable T/APC contacts by inducing the conformational change of LFA-1 to a high binding state. We tested this hypothesis using a laminar flow chamber. Our experimental model proved CCL19 to have little or no influence on the naive T cell adhesion to mDC and no effect on the stability of the contact, once established. These results are not unprecedented. On the luminal surface of HEVs, CCL21 activates LFA-1 and is essential for the firm arrest of rolling T cells (28, 29). Once the T cells have entered the lymph nodes via diapedesis, however, the higher LFA-1/ICAM-1 affinity can be triggered by a chemokine-independent mechanism that requires the engagement of other surface receptors, such as the TCR (30). In addition, the T/DC adhesion process would be controlled by multiple redundant mechanisms. Abrogating the contribution of CCL19 could not be sufficient to inhibit the conjugates formed between naive T cells and mDCs.

CCL19 could also lower the threshold of activation of naive T cells, thereby increasing their sensitivity to low density Ag presentation. In fact, several chemokines, including CXCL12, have been shown to up-regulate CD4 T cell proliferation induced by TCR engagement (31). We tested this hypothesis by assuming that a decreased threshold of activation would allow for a higher frequency of Ca²⁺-responding T cells as well as for more intense or more sustained Ca²⁺ transients. In contact experiments, we observed a difference in the frequency (Figs. 1f and 3e), but not in the amplitude of the Ag-independent Ca²⁺ responses obtained with DCs after adding or blocking CCR7 signaling. To further assess a potential synergy of CCL19 on Ag-specific Ca²⁺ responses, we used suboptimal concentrations of anti-CD3 mAb coated on plates or of the superantigen staphylococcal enterotoxin E. No significant effect of CCR7 signaling on the frequency or amplitude of naive T cell Ca²⁺ responses could be observed in those settings (data not shown). These results suggest that CCL19 does not directly lower the threshold of T cell activation through the TCR/CD3 complex.

This chemokine is, however, likely to exert an indirect effect on the sensitization of naive T cells. Indeed, CCL19 triggers T cell polarization, which is characterized by accumulation of adhesion, costimulatory, and signaling molecules at the leading edge, with exclusion of molecules that impair cell-cell contacts, such as CD43 (32). We found that naive T cell polarization is correlated with an increased frequency of Ag-independent Ca²⁺ responses (Fig. 1, b and e). Therefore, CCL19 may indirectly lower the threshold of T cell activation by first improving the ability of the T cells to interact with APCs and then by making this interaction more dynamic.

Moreover, Ag-independent T/DC interaction has been shown to induce phosphorylation of CD3ζ, an early TCR signaling indicator (10). In other words, Ag-independent responses could lower the threshold of T cell activation by triggering a preactivated state that is nurtured by serial T/APC encounters (26). In murine lymph nodes, Ag-independent TCR stimulation, relying on self-MHC molecules, can facilitate T cell responses to foreign Ag (33).

CCL19 induces a strong motility of naive T cells, the basis for the serial encounters between T cells and multiple DCs (the present study and Refs. 5 and 26). In the absence of Ag, serial T/DC encounters and the resulting Ca^{2+} transients were shown to increase T cell survival in vitro (10, 11). However, the role of CCL19 in DC-induced T cell survival in vivo awaits further investigations. CCL19 can also deliver antiapoptotic signals to DCs (34).

The motility of polarized cells facilitates the stochastic encounter of naive T cells with their rare cognate Ag-bearing APCs (Fig. 5). Moreover, CCL19 induces the formation and wider spreading of dendrites in DCs (35), which may further increase the chances of T/APC interaction.

What is the physiological relevance of these results?

CCL19 is essential in our experimental conditions, where the chemokines secreted by mDCs are the only ones to influence the behavior of naive T cells. In vivo, other chemokines, such as CXCL12, CCL21, and CCL18, can affect naive T cells. We observed that rCXCL12, but not CCL18, was able to increase the motility and frequency of Ca^{2+} responses of naive T cells to iDCs at least as efficiently as rCCL19 or CCL21. It is important, however, to consider the in vivo compartmentalization of these chemokines; in the lymph nodes, CCL21 and CXCL12 are secreted at the level of HEVs, whereas only CCL19 and CCL21 are present at the level of the T cell areas (36, 37).

In the steady state, most resident DCs in murine lymph nodes are immature (38), and stromal cells constitutively secrete CCL19 and CCL21. Both these chemokines could be important for the interaction between naive T cells and the resident immature DCs.

When a danger signal occurs, the relative importance of CCL19 secreted by mDCs or reticular stromal cells in T cell areas is unclear. A recent immunohistochemistry study in human lymph nodes indicates that mDCs and not stromal cells are the main source of CCL19. DCs in contact with naive T cells were shown to secrete CCL19, but not CCL21 (21). This may be sufficient to account for a preferential scanning of the mDCs by the incoming naive T cells (22). The influx of mDCs is expected to increase the intranodal concentration of CCL19, allowing this chemokine to be displayed on the luminal surface of the HEVs by transcytosis (28, 39). The HEV-bound chemokine will help to recruit more naive T cells from the blood and thus augment the chances for specific T cells to find their cognate Ag.

Finally, injection of maturing DC in the context of immunotherapy protocols may induce a local inflammation with a high concentration of CCL19. Together with the inflammatory signals, the local CCL19 accumulation could stimulate the recruitment of naive T cells at the site of injection and the formation of tertiary lymphoid structures, a lymphoid-like organization composed of DCs, lymphocytes, HEVs, and stromal cells. These structures appear upon ectopic expression of CCL19 in mice pancreatic islets or chronically inflamed tissues (36, 40). Within this context, T cell priming could occur.

T cell random motility in murine lymph nodes has been previously observed and finely characterized (5, 6). However, the molecular mechanisms leading to such exploratory behavior have not been clarified. Chemokines are usually considered more likely to induce directional cell migration, rather than random movements. We here show that a chemokine regulates this activity in human naive T cells. Although CCR7 and its ligands are expected to attract naive T cells and mature DCs in lymph nodes, once in the T cell areas the main effect of CCL19 (and possibly CCL21) is to maintain a high random motility of polarized T cells as well as DC dendrite spreading. These phenomena favor the occurrence of Ag-

independent responses and increase the probability of cognate MHC-peptide encounter.

Acknowledgments

We thank Dr. F. Heshmati of the Cochin Hospital Transfusion Center (Paris, France) for his essential assistance with the apheresis procedure; A. Boyer, C. Bardon, C. Cambouris, I. Chauvet, H. Keller, K. Labroquère, M. L. Lefebvre, and S. Martin for skillful DC preparation; and M. Salcedo and E. Mallard for discussion.

Disclosures

The authors have no financial conflict of interest.

References

- Banchereau, J., and R. M. Steinman. 1998. Dendritic cells and the control of immunity. *Nature* 392: 245–252.
- Constantin, G., M. Majeed, C. Giagulli, L. Piccio, J. Y. Kim, E. C. Butcher, and C. Laudanna. 2000. Chemokines trigger immediate β_2 integrin affinity and mobility changes: differential regulation and roles in lymphocyte arrest under flow. *Immunity* 13: 759–769.
- Luther, S. A., H. L. Tang, P. L. Hyman, A. G. Farr, and J. G. Cyster. 2000. Coexpression of the chemokines ELC and SLC by T zone stromal cells and deletion of the ELC gene in the *plt/plt* mouse. *Proc. Natl. Acad. Sci. USA* 97: 12694–12699.
- Vassileva, G., H. Soto, A. Zlotnik, H. Nakano, T. Kakiuchi, J. A. Hedrick, and S. A. Lira. 1999. The reduced expression of 6Ckine in the *plt* mouse results from the deletion of one of two 6Ckine genes. *J. Exp. Med.* 190: 1183–1188.
- Mempel, T. R., S. E. Henrickson, and U. H. Von Andrian. 2004. T-cell priming by dendritic cells in lymph nodes occurs in three distinct phases. *Nature* 427: 154–159.
- Miller, M. J., A. S. Hejazi, S. H. Wei, M. D. Cahalan, and I. Parker. 2004. T cell repertoire scanning is promoted by dynamic dendritic cell behavior and random T cell motility in the lymph node. *Proc. Natl. Acad. Sci. USA* 101: 998–1003.
- Miller, M. J., S. H. Wei, M. D. Cahalan, and I. Parker. 2003. Autonomous T cell trafficking examined in vivo with intravital two-photon microscopy. *Proc. Natl. Acad. Sci. USA* 100: 2604–2609.
- Bouso, P., and E. Robey. 2003. Dynamics of CD8⁺ T cell priming by dendritic cells in intact lymph nodes. *Nat. Immunol.* 4: 579–585.
- Real, E., A. Kaiser, G. Raposo, A. Amara, A. Nardin, A. Trautmann, and E. Donnadieu. 2004. Immature dendritic cells (DCs) use chemokines and intercellular adhesion molecule (ICAM)-1, but not DC-specific ICAM-3-grabbing nonintegrin, to stimulate CD4⁺ T cells in the absence of exogenous antigen. *J. Immunol.* 173: 50–60.
- Kondo, T., I. Cortese, S. Markovic-Plese, K. P. Wandinger, C. Carter, M. Brown, S. Leitman, and R. Martin. 2001. Dendritic cells signal T cells in the absence of exogenous antigen. *Nat. Immunol.* 2: 932–938.
- Revy, P., M. Sospedra, B. Barbour, and A. Trautmann. 2001. Functional antigen-independent synapses formed between T cells and dendritic cells. *Nat. Immunol.* 2: 925–931.
- Goxe, B., N. Latour, M. Chokri, J. P. Abastado, and M. Salcedo. 2000. Simplified method to generate large quantities of dendritic cells suitable for clinical applications. *Immunol. Invest.* 29: 319–336.
- Boccaccio, C., S. Jacod, A. Kaiser, A. Boyer, J. P. Abastado, and A. Nardin. 2002. Identification of a clinical-grade maturation factor for dendritic cells. *J. Immunother.* 25: 88–96.
- Donnadieu, E., G. Bismuth, and A. Trautmann. 1994. Antigen recognition by helper T cells elicits a sequence of distinct changes of their shape and intracellular calcium. *Curr. Biol.* 4: 584–595.
- Gryniewicz, G., M. Poenie, and R. Y. Tsien. 1985. A new generation of Ca^{2+} indicators with greatly improved fluorescence properties. *J. Biol. Chem.* 260: 3440–3450.
- Delon, J., N. Bercovici, G. Raposo, R. Liblau, and A. Trautmann. 1998. Antigen-dependent and -independent Ca^{2+} responses triggered in T cells by dendritic cells compared with B cells. *J. Exp. Med.* 188: 1473–1484.
- Adema, G. J., F. Hartgers, R. Verstraten, E. de Vries, G. Marland, S. Menon, J. Foster, Y. Xu, P. Nooyen, T. McClanahan, et al. 1997. A dendritic-cell-derived C-C chemokine that preferentially attracts naive T cells. *Nature* 387: 713–717.
- Langenkamp, A., K. Nagata, K. Murphy, L. Wu, A. Lanzavecchia, and F. Sallusto. 2003. Kinetics and expression patterns of chemokine receptors in human CD4⁺ T lymphocytes primed by myeloid or plasmacytoid dendritic cells. *Eur. J. Immunol.* 33: 474–482.
- Sallusto, F., B. Palermo, D. Lenig, M. Miettinen, S. Matikainen, I. Julkunen, R. Forster, R. Burgstahler, M. Lipp, and A. Lanzavecchia. 1999. Distinct patterns and kinetics of chemokine production regulate dendritic cell function. *Eur. J. Immunol.* 29: 1617–1625.
- Vissers, J. L., F. C. Hartgers, E. Lindhout, M. B. Teunissen, C. G. Figdor, and G. J. Adema. 2001. Quantitative analysis of chemokine expression by dendritic cell subsets in vitro and in vivo. *J. Leukocyte Biol.* 69: 785–793.
- Katou, F., H. Ohtani, T. Nakayama, H. Nagura, O. Yoshie, and K. Motegi. 2003. Differential expression of CCL19 by DC-Lamp⁺ mature dendritic cells in human lymph node versus chronically inflamed skin. *J. Pathol.* 199: 98–106.
- Benvenuti, F., C. Lagaudriere-Gesbert, I. Grandjean, C. Jancic, C. Hivroz, A. Trautmann, O. Lantz, and S. Amigorena. 2004. Dendritic cell maturation

- controls adhesion, synapse formation, and the duration of the interactions with naive T lymphocytes. *J. Immunol.* 172: 292–301.
23. Forster, R., A. Schubel, D. Breitfeld, E. Kremmer, I. Renner-Muller, E. Wolf, and M. Lipp. 1999. CCR7 coordinates the primary immune response by establishing functional microenvironments in secondary lymphoid organs. *Cell* 99: 23–33.
 24. Gunn, M. D., S. Kyuwa, C. Tam, T. Kakiuchi, A. Matsuzawa, L. T. Williams, and H. Nakano. 1999. Mice lacking expression of secondary lymphoid organ chemokine have defects in lymphocyte homing and dendritic cell localization. *J. Exp. Med.* 189: 451–460.
 25. Ngo, V. N., H. L. Tang, and J. G. Cyster. 1998. Epstein-Barr virus-induced molecule 1 ligand chemokine is expressed by dendritic cells in lymphoid tissues and strongly attracts naive T cells and activated B cells. *J. Exp. Med.* 188: 181–191.
 26. Gunzer, M., A. Schafer, S. Borgmann, S. Grabbe, K. S. Zanker, E. B. Brocker, E. Kampgen, and P. Friedl. 2000. Antigen presentation in extracellular matrix: interactions of T cells with dendritic cells are dynamic, short lived, and sequential. *Immunity* 13: 323–332.
 27. Pilkington, K. R., I. Clark-Lewis, and S. R. McColl. 2004. Inhibition of generation of cytotoxic T lymphocyte activity by a CCL19/macrophage inflammatory protein (MIP)-3 β antagonist. *J. Biol. Chem.* 279: 40276–40282.
 28. Stein, J. V., A. Rot, Y. Luo, M. Narasimhaswamy, H. Nakano, M. D. Gunn, A. Matsuzawa, E. J. Quackenbush, M. E. Dorf, and U. H. von Andrian. 2000. The CC chemokine thymus-derived chemotactic agent 4 (TCA-4, secondary lymphoid tissue chemokine, 6CKine, exodus-2) triggers lymphocyte function-associated antigen 1-mediated arrest of rolling T lymphocytes in peripheral lymph node high endothelial venules. *J. Exp. Med.* 191: 61–76.
 29. Weninger, W., H. S. Carlsen, M. Goodarzi, F. Moazed, M. A. Crowley, E. S. Baekkevold, L. L. Cavanagh, and U. H. von Andrian. 2003. Naive T cell recruitment to nonlymphoid tissues: a role for endothelium-expressed CC chemokine ligand 21 in autoimmune disease and lymphoid neogenesis. *J. Immunol.* 170: 4638–4648.
 30. Bromley, S. K., and M. L. Dustin. 2002. Stimulation of naive T-cell adhesion and immunological synapse formation by chemokine-dependent and -independent mechanisms. *Immunology* 106: 289–298.
 31. Nanki, T., and P. E. Lipsky. 2000. Cutting edge: stromal cell-derived factor-1 is a costimulator for CD4⁺ T cell activation. *J. Immunol.* 164: 5010–5014.
 32. Friedl, P., and M. Gunzer. 2001. Interaction of T cells with APCs: the serial encounter model. *Trends Immunol.* 22: 187–191.
 33. Stefanova, I., J. R. Dorfman, and R. N. Germain. 2002. Self-recognition promotes the foreign antigen sensitivity of naive T lymphocytes. *Nature* 420: 429–434.
 34. Sanchez-Sanchez, N., L. Riol-Blanco, G. de la Rosa, A. Puig-Kroger, J. Garcia-Bordas, D. Martin, N. Longo, A. Cuadrado, C. Cabanas, A. L. Corbi, et al. 2004. Chemokine receptor CCR7 induces intracellular signaling that inhibits apoptosis of mature dendritic cells. *Blood* 104: 619–625.
 35. Yanagawa, Y., and K. Onoe. 2002. CCL19 induces rapid dendritic extension of murine dendritic cells. *Blood* 100: 1948–1956.
 36. Luther, S. A., A. Bidgol, D. C. Hargreaves, A. Schmidt, Y. Xu, J. Paniyadi, M. Matloubian, and J. G. Cyster. 2002. Differing activities of homeostatic chemokines CCL19, CCL21, and CXCL12 in lymphocyte and dendritic cell recruitment and lymphoid neogenesis. *J. Immunol.* 169: 424–433.
 37. von Andrian, U. H., and T. R. Mempel. 2003. Homing and cellular traffic in lymph nodes. *Nat. Rev. Immunol.* 3: 867–878.
 38. Wilson, N. S., D. El-Sukkari, G. T. Belz, C. M. Smith, R. J. Steptoe, W. R. Heath, K. Shortman, and J. A. Villadangos. 2003. Most lymphoid organ dendritic cell types are phenotypically and functionally immature. *Blood* 102: 2187–2195.
 39. Baekkevold, E. S., T. Yamanaka, R. T. Palframan, H. S. Carlsen, F. P. Reinholt, U. H. von Andrian, P. Brandtzaeg, and G. Haraldsen. 2001. The CCR7 ligand elc (CCL19) is transcytosed in high endothelial venules and mediates T cell recruitment. *J. Exp. Med.* 193: 1105–1112.
 40. Hjelmstrom, P. 2001. Lymphoid neogenesis: de novo formation of lymphoid tissue in chronic inflammation through expression of homing chemokines. *J. Leukocyte Biol.* 69: 331–339.